Increments of Progress Towards Air Quality Objectives - ODSVRA Dust Controls

J.A. Gillies, E. Furtak-Cole, V. Etyemezian

Dust controls including temporary wind fences and vegetation projects have been used within the ODSVRA to reduce the emissions of PM_{10} originating from the ODSVRA, reduce the mass emissions of PM_{10}, and lower the regional PM_{10} burden. Beginning in 2014, 28 acres of dust controls were put into place and the amount of acreage has increased through to 223 acres in 2020. The position of these control areas to date in the ODSVRA have favored locations that should, according to model results, reduce the PM_{10} measured at CDF, but the expectation is that the benefit to air quality will be felt over a wider area, as illustrated in Fig. 1. In 2021, an additional 90 acres of dust control will be established in the ODSVRA, at positions that should reduce the PM_{10} burden further south and result in measured decreases in PM_{10} concentration at Mesa2. The model results indicate that the presence of the dust control areas in 2020 reduce the PM_{10} levels for the CDF measurement station as shown in Fig. 1 by ≈50%, assuming the controls are 100% effective.

Here we demonstrate that the PM_{10} data measured at CDF and wind data measured at CDF and the S1 tower, show that the dust emission system in that part of the ODSVRA where controls have been placed, produces less PM_{10} now than it did prior to the emplacement of those controls and that this reduction in PM_{10} scales with the increase in acres of dust control.
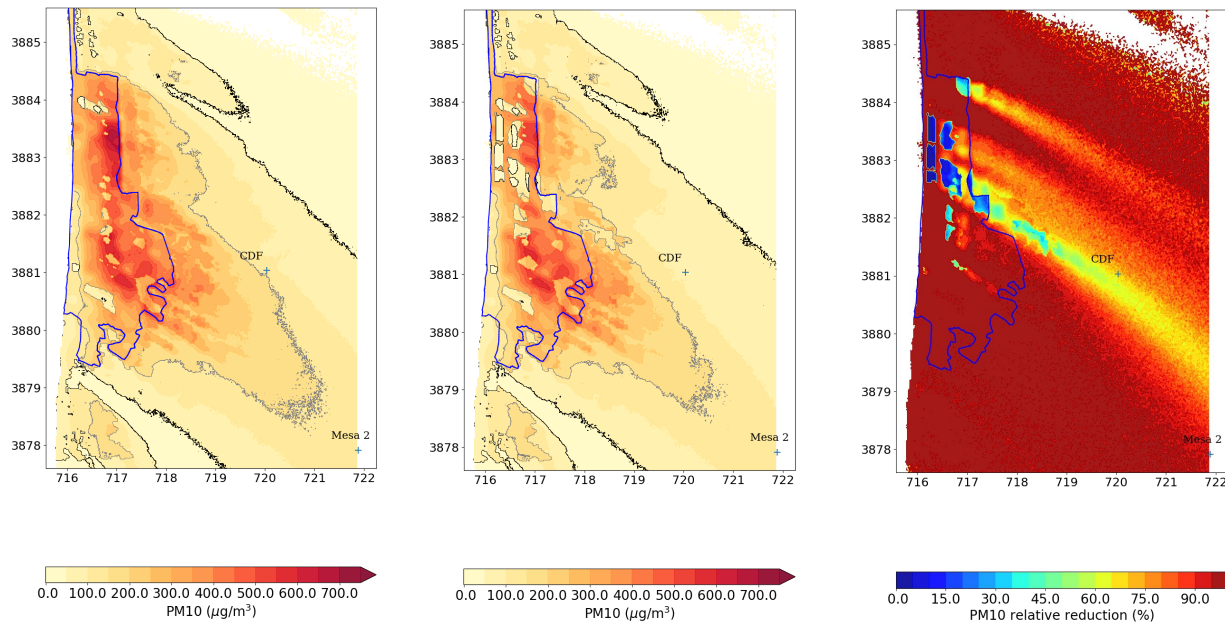

Figure 1. Modeled PM_{10} concentration maps for the 10 baseline days of 2013 for the case of no controls (left panel) and for the controls in place in 2020 (middle panel). The panel on the right shows the percent change in the PM_{10} between 2013 and 2020 due to the reduction in emissions created by the dust controls. The black line in the maps surrounds the area wherein the 24 hour mean PM_{10} concentration is >50 µg m^{-3} indicating it is above the State standard and the grey line surrounds the area wherein the 24 hour mean PM_{10} concentration is >150 µg m^{-3} indicating it is above the Federal standard.

Furtak-Cole and Gillies in their memo of 10/27/2020 demonstrated that PM_{10} as measured at CDF is strongly linked to the wind power density (WPD, W m^{-2}) quantified at the S1 tower in the ODSVRA for the months of May and June (Fig. 2) based on the mean hourly data record of 2011 to 2020. Wind power density (WPD) is defined as (e.g., Kalmikov, 2017):

WPD=0.5 ρ_a u^3 (1)

where ρ_a is air density (kg m^{-3}), and u (m s^{-1}) is wind speed at 10 m above ground level (AGL) common to all three sites.

We build on the work of Furtak-Cole and Gillies (2020) to examine the seasonality of total WPD (i.e., Jan-March [J-M], April-June [A-J], July-September [J-S], and October to December [O-D]) measured at CDF, Mesa2, and S1 and its relation to total PM_{10} at CDF and Mesa2. The summations of PM_{10} and WPD for each season are based on filtering the data for wind direction, a threshold wind speed and a moisture condition. The following steps were taken:

1) Winds from 248° to 326° are used to ensure, conservatively, that the air flow that reaches CDF and Mesa2 has most likely travelled from the ODSVRA.
2) A wind speed filter is applied based on screening for the conditions where it is most likely that the PM_{10} reaching CDF and Mesa2 is due to the generation of dust by the saltation process within the ODSVRA.
3) We adopt the threshold wind speeds for CDF, Mesa2, and S1 tower as derived by Furtak-Cole and Gillies, i.e., S1 tower wind data below a mean hourly value of 8 m s^{-1} at 10 m above ground level (AGL) are removed and for CDF and Mesa2 we filter the wind speed and PM_{10} data removing all hourly data when wind speeds at 10 m AGL are <4.5 m s^{-1} (Fig. 3).

We apply one additional filter to try and account for an important source of moisture that will affect the threshold wind shear for saltation and the strength of the dust emissions (Bauer et al., 2009; Nield and Wiggs, 2011; Ishizuka et al., 2008; Munkhtsetseg et al., 2016).

4) We eliminate hourly wind speed and the corresponding PM_{10} data for that hour if there has been a precipitation event from one to three days prior to the measurement (precipitation data from San Luis Obispo airport and a nearby National Weather Service station).

It is important to recognize that PM_{10} concentration and WPD are summed over the same filtered-hours. Therefore, the removal of days with potentially elevated moisture conditions (precipitation recorded within the last three days) may affect the total WPD, but not the correlation of these two quantities. In seeking a correlation, it is better to err on the side of removing too much data, than having the relation biased by hours when moist sand strongly influences the production of PM_{10} under saltation-strength winds.

Results

Seasonality of Wind Power Density

WPD as a function of season for CDF, Mesa2, and S1 for the period 2011-2020 are shown in Fig. 4. The temporal pattern of WPD as a function of season is preserved across the three sites, which indicates that the broad wind speed patterns are similar across the domain for each season. As expected, the highest WPD is observed in A-J when dust emission and transport is most likely.
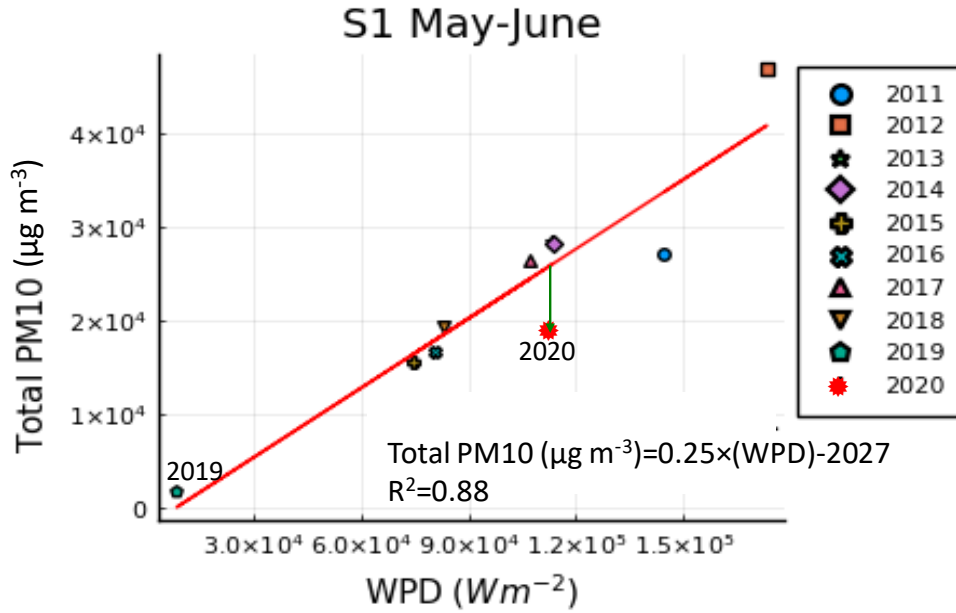
Figure 2. Total PM_{10} ($\mu g\ m^{-3}$) at CDF and total WPD (W m^{-2}) at S1 for the months May and June, 2011-2020 (from Furtak-Cole and Gillies, 2020).
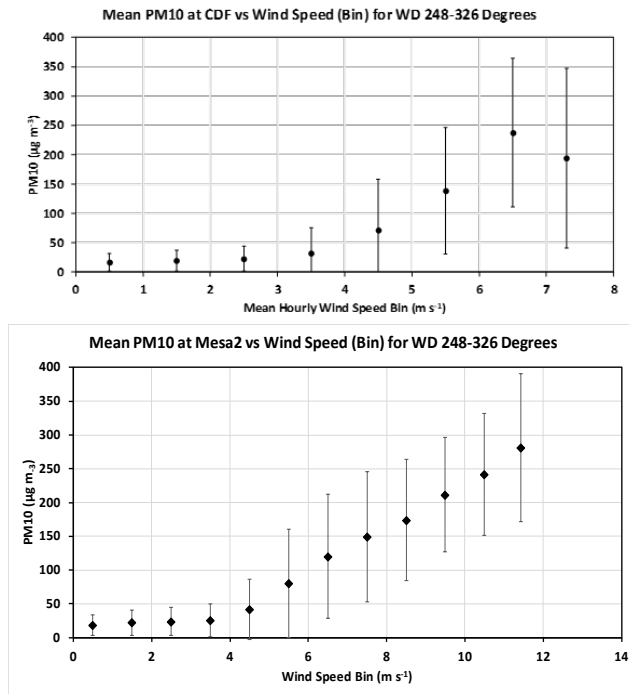

Figure 3. The relation between hourly mean PM_{10} and hourly mean wind speed measured at 10 m AGL for winds from 248°-326° observed at CDF in in 2019 (Jan-Dec) and Mesa2 for 2009-2020. PM_{10} increases as a function of wind speed bin for bins ≥4.5 m s^{-1}.

Total PM_{10} and Total WPD Seasonal Relations

Furtak-Cole and Gillies (2020) demonstrated that Total WPD measured at CDF and S1 was correlated with Total PM_{10} at CDF for the months May and June for the period 2011-2020 (Fig. 2). This relation is

also observed, by season, using the total PM and wind data at CDF and Mesa2 (Fig. 4) and between WPD at S1 and total PM_{10} at CDF and Mesa2. Fig. 5 show this relation for total PM_{10} by season for CDF and Mesa2 and total WPD at S1.
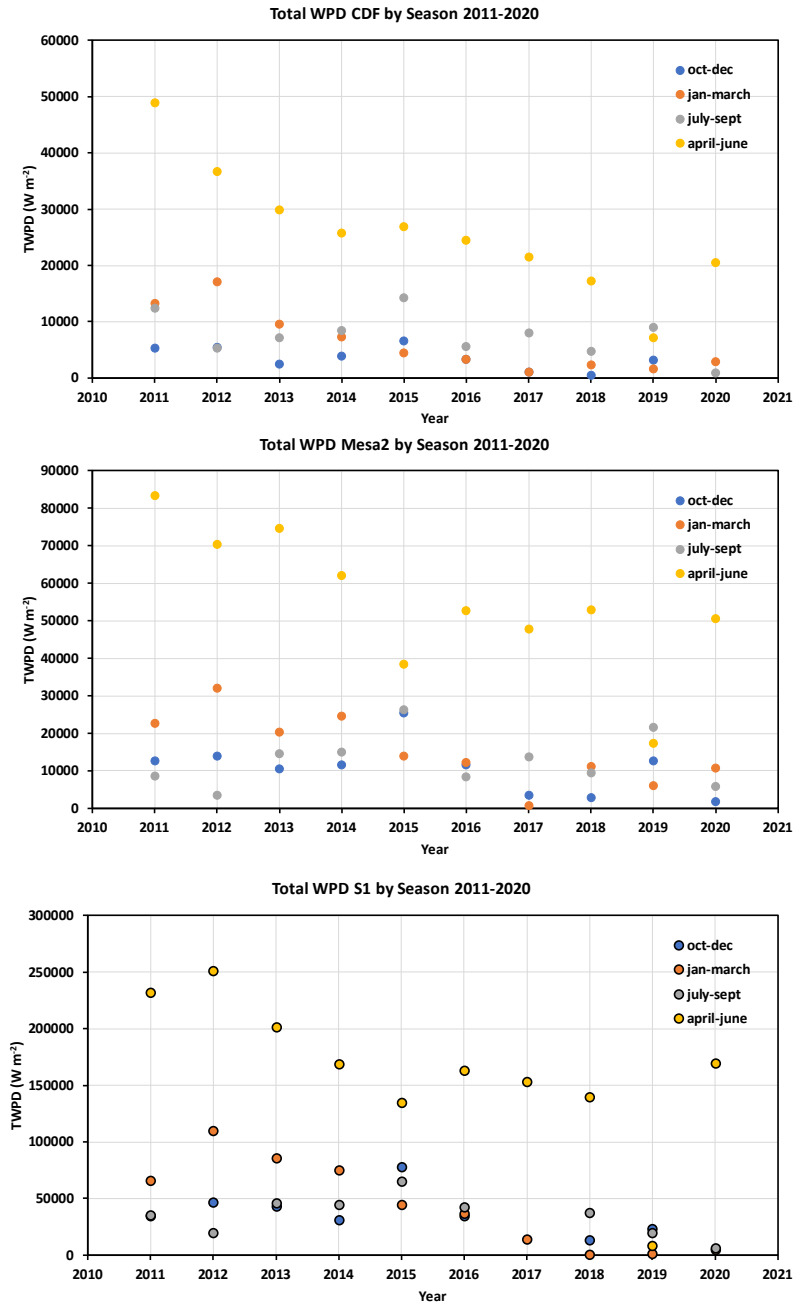

Figure 4. Total WPD (W m^{-2}) at CDF (top panel), Mesa2 (middle panel) and S1 (bottom panel) as a function of season for the period 2011-2020, after applying the direction, wind speed, and moisture filters.
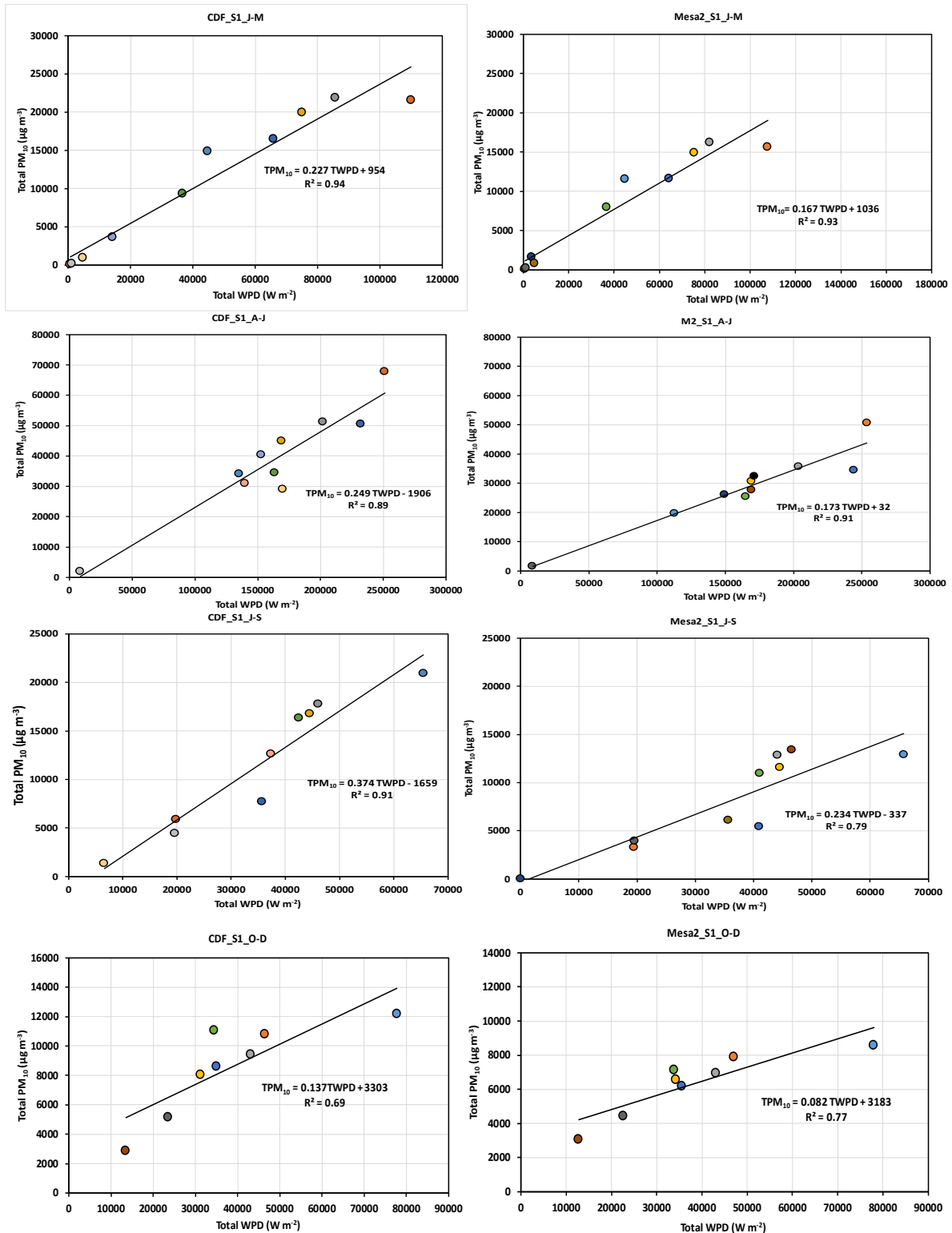
Figure 5. Total PM$_{10}$ (µg m^{-3}) at CDF (left panels) and Mesa2 (right panels) as a function of total WPD (W m^{-2}) at S1, by season for the period 2011-2020 after applying the direction, wind speed, and moisture filters. The different colors of the circles represent the years from 2011 to 2020.

During spring and summer the dust emission system is typically most active at the ODSVRA and the combined A-J and J-S data for total PM_{10} for CDF and Mesa2 and total WPD from S1 shows a high degree of correlation (Fig. 6).
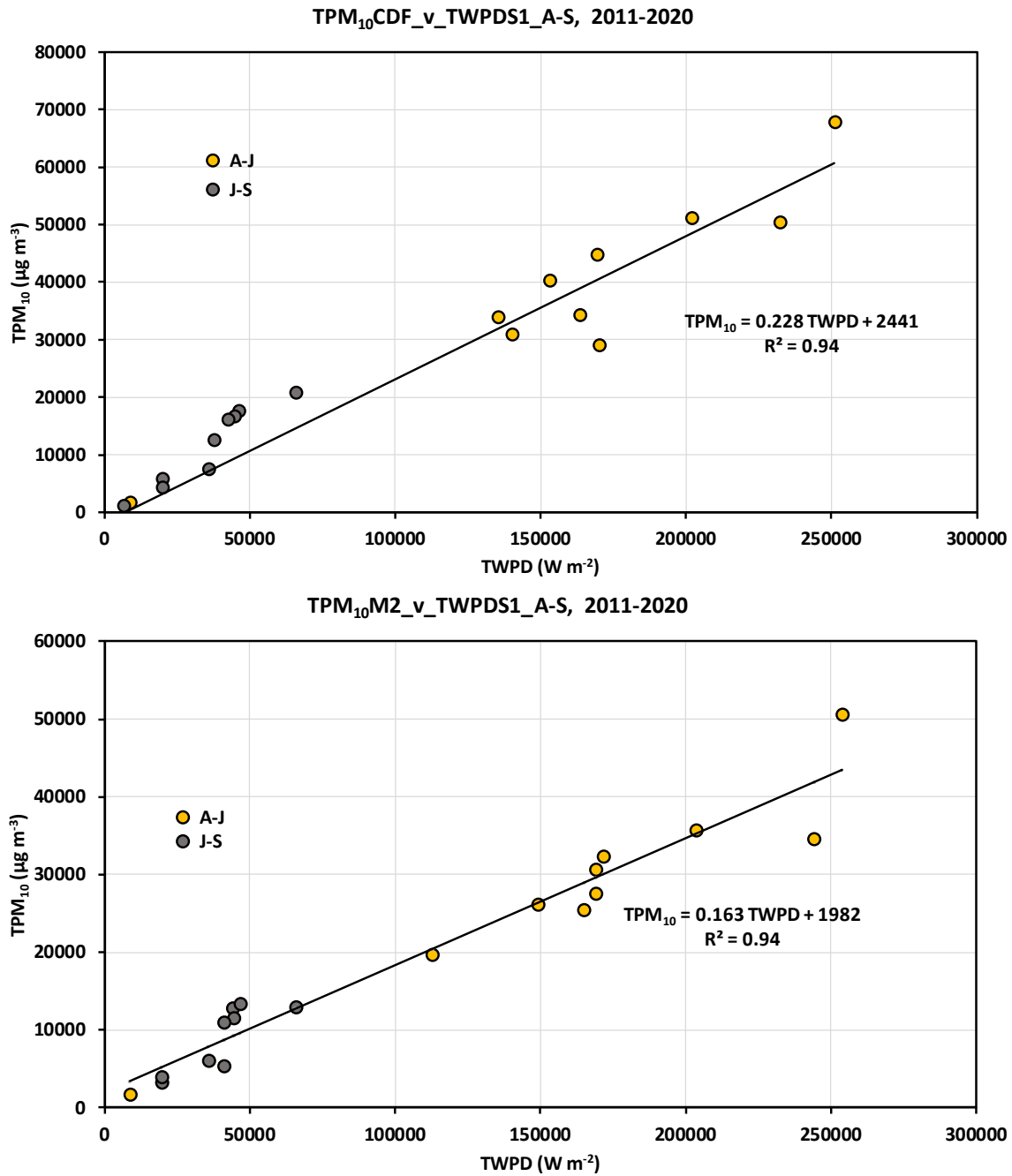
$TPM_{10}CDF\_v\_TWPDS1\_A-S$, 2011-2020

$$TPM_{10} = 0.228\ TWPD + 2441$$
$$R^2 = 0.94$$

$TPM_{10}M2\_v\_TWPDS1\_A-S$, 2011-2020

$$TPM_{10} = 0.163\ TWPD + 1982$$
$$R^2 = 0.94$$

Figure 6. Total PM_{10} as a function of total WPD for the combined spring and summer period (i.e., April-September) for CDF and S1 tower (top panel) and Mesa2 and S1 tower (bottom panel).

As Figs. 5 and 6 demonstrate the PM$_{10}$ response at CDF and Mesa2 is highly correlated with the WPD within the ODSVRA as characterized by the S1 tower wind speed measurements. This suggests that the ratio of total PM$_{10}$:total WPD can serve as a metric to evaluate how the dust emission system is changed by changes to the landscape. With no changes to the surface where the emissions originate from, this ratio will reflect the efficiency of the wind and saltation system to produce PM$_{10}$ for the prevailing environmental conditions during the period of interest. If, however, the surface from which the emissions are originating from is being systematically altered, for example, by altering the size of the source area by applying dust controls, the ratio should diminish as more area is removed from dust production. For an equivalent WPD there should be less PM$_{10}$ being produced due to the reduction in source area. There is a limit to the explanatory power of this ratio, which is that if winds are at or close to the designated threshold speed either at the monitoring location or in the source area for a large part of the record (observed most often in fall and winter), the value becomes unstable due to a potential paucity of data but also because as wind speed diminishes the strength of the coupling between the wind and the saltation-generated PM$_{10}$ weakens and is subject to influence of PM$_{10}$ from other sources.

Based on the number of acres of dust control that have been established from 2011 through 2020, Fig. 7 shows that at CDF for the period April through September there has been a downward trend in the TPM$_{10}$:TWPD ratio with increasing amounts of dust control acreage, with the caveat that the data from 2019 were removed because there were few hours where the winds exceeded the threshold wind speed (i.e., an unstable ratio condition). The lowest values of this ratio were observed in the spring and summer of 2020, which coincidentally is the year that OHV activity at the ODSVRA was restricted. This raises the question as to whether the ratio is low due to dust controls or due to the cessation of OHV activity that could indicate that there had been a reduction in emissivity.
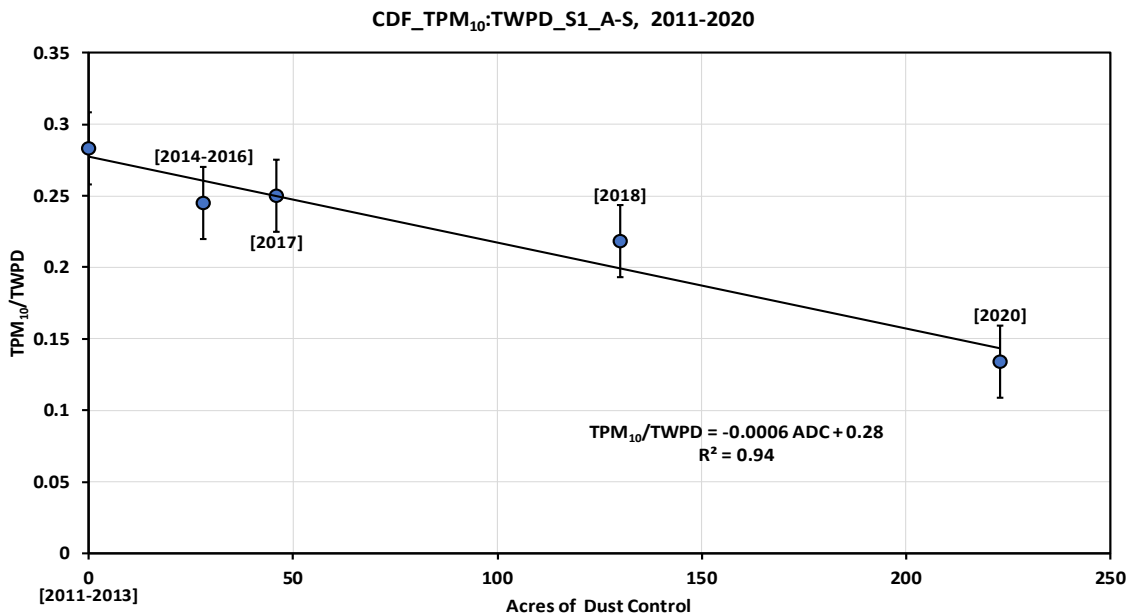

CDF_TPM$_{10}$:TWPD_S1_A-S, 2011-2020

$TPM_{10}/TWPD = -0.0006 \, ADC + 0.28$
$R^2 = 0.94$

Figure 7. The relation between the TPM$_{10}$:TWPD ratio and the acres of dust control for the CDF total PM$_{10}$ data and the S1 total WPD data from 2011-2020 for the April through September period. Dates for the amounts of acres of dust control are shown in parentheses and the error bars represent the Standard Error (std d/(#obs-1)^2).

The total PM_{10} data from Mesa2 and WPD data from S1 can provide some indication whether the low ratio observed in 2020 at CDF was due to dust controls or a change in emissivity. The ratio of TPM_{10}:TWPD for Mesa2 and S1 data for the period April through September as a function of acres of dust control is shown in Fig. 8. This figure shows that, unlike CDF, there has been no downward trend in the TPM_{10}:TWPD ratio with increasing acres of dust control (2019 data also removed). The dispersion modeling results shown in Fig. 1 support this as it shows that the PM_{10} levels at Mesa2 decrease by approximately 7% (compared to 42% modeled reduction at CDF) with the presence of the dust controls that are mostly upwind of CDF in 2020, compared to the baseline condition of 2013. That there has been no change in the TPM_{10}:TWPD at Mesa2 with increasing acres of dust control could be an indication that at CDF the decrease in the ratio by 2020 is due to the presence of the dust controls and not a change in the surface emissivity. If that were the case a concomitant decrease in this ratio at Mesa2 in 2020 should have been observed. It needs to be noted, however, that there is more area upwind of Mesa2 that is non-riding compared to CDF, so that the cessation of riding would have a proportionately smaller effect.

Figure 7 suggests that the emplacement of the dust controls upwind of CDF have reduced the production of PM_{10} by 48% for equivalent WPD for the no-control conditions 2011-2013 versus 2020. This is in line with the 42% reduction in mean PM_{10} at CDF predicted by the DRI Lagrangian particle dispersion model with the 223 acres set to zero emissions. Figures 7 and 8 suggest that a change in emissivity due to the cessation of riding was likely not the causal mechanism resulting in a lower ratio at CDF as this should have resulted in a lower ratio at Mesa2 at least to a value less than the mean (0.19) minus one standard deviation (0.05), to provide some confidence that it was a real reduction.

In 2021 an additional 90 acres of dust control are to be placed in the ODSVRA upwind of Mesa2. The effect on PM_{10} at Mesa2, as predicted by the DRI dispersion model, is a reduction between 26%-28%
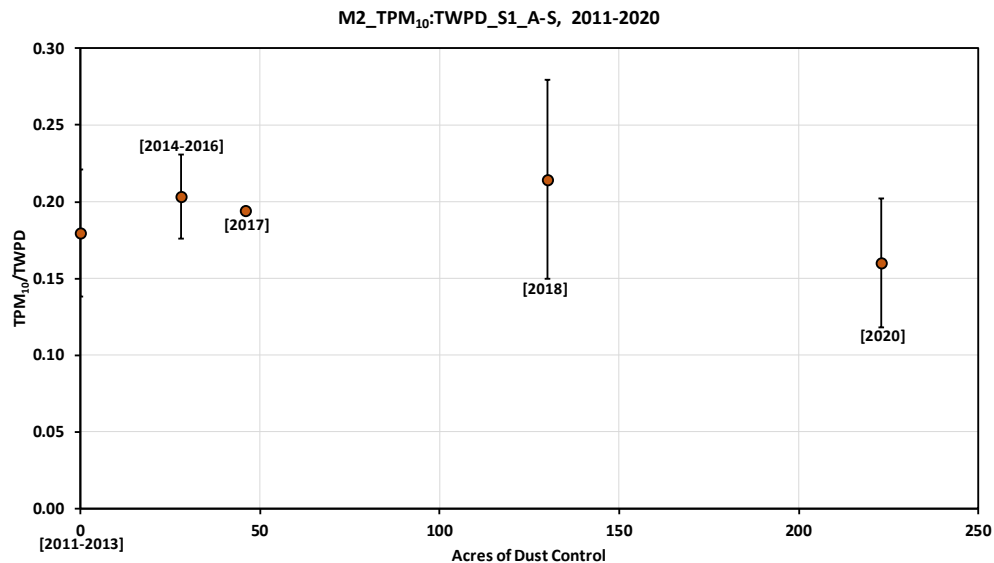

Figure 8. The relation between the TPM_{10}:TWPD ratio and the acres of dust control for the Mesa2 total PM_{10} data and the S1 total WPD data from 2011-2020 for the April through September period. Dates for the amounts of acres of dust control are shown in parentheses and the error bars represent the Standard Error (std d/(#obs-1)^2).

depending on which of two options under consideration are chosen. If we assume that 90 acres of control would have the same effect on Mesa2 as it does on CDF with respect to reducing the TPM_{10}:TWPD value, the ratio value should be approximately 0.15 in 2021, assuming all other environmental conditions are equal.

This analysis has demonstrated that total WPD measured at the S1 tower is a powerful metric for explaining the relationship between wind-driven saltation and the accompanying emission of mineral dust PM_{10} from the ODSVRA as measured at two key receptor sites, CDF and Mesa2. Its strength, in part, is also due to the relatively low degree of restrictions on the input data unlike earlier methods that have relied on highly restrictive environmental conditions as, for example, by the "Zeldin approach", which creates quite small data sets.

The TWPD and TPM_{10} measurement-based metric indicates, along with the dispersion modeling, that the PM_{10} originating from the ODSVRA has been reduced by the dust controls by approximately 45%. It also demonstrates that the TPM_{10}:TWPD ratio can be used to track the progress of the effect of dust controls on the dust emission system within the ODSVRA to quantify increments of progress as management efforts to limit the dust emissions are further developed to meet the SOA. It needs to be noted that the TPM_{10}:TWPD ratio indicates the production potential of PM_{10} as a function of WPD and an increase in WPD can result in more exceedances of the State or Federal standard even in the presence of increased amounts of dust controls because the PM_{10} is produced from the uncontrolled areas and it increases as a power function of wind speed, while the efficiency of the dust control does not.

References

Bauer, B.O., R.G.D. Davidson-Arnott, P.A. Hesp, S.L. Namikas, J. Ollerhead & I.J. Walker (2009) Aeolian sediment transport on a beach: Surface moisture, wind fetch, and mean transport. *Geomorphology,* 105**,** 106-116.

Ishizuka, M., M. Mikami, J. Leys, Y. Yamada, S. Heidenreich, Y. Shao & G.H. McTainsh (2008) Effects of soil moisture and dried raindroplet crust on saltation and dust emission. *Journal of Geophysical Research,* 113.

Kalmikov, A. 2017. Wind power fundamentals. In *Wind Power Engineering,* ed. T.M. Letcher. Elsevier Science Publishing Co., Inc.

Munkhtsetseg, E., M. Shinoda, J.A. Gillies, R. Kimura, J. King & G. Nikolich (2016) Relationships between soil moisture and dust emissions in a bare sandy soil of Mongolia. *Particuology*, 28, 131-137.

Nield, J.M. & G.F.S. Wiggs (2011) The application of terrestrial laser scanning to aeolian saltation cloud measurement and its response to changing surface moisture. *Earth Surface Processes and Landforms,* 36**,** 273-278.